Novel Experimental Techniques and Realizations of Quasi-Periodicity

P.M. Chaikin[1,2], *A. Behrooz*[1], *M.J. Burns*[1,3], *D. Levine*[1,5], *D. Ou-Yang*[1,2], *B. Whitehead*[4], *and X. Yan*[1]

[1]Dept. of Physics and Laboratory for Research on the Structure of Matter, University of Pennsylvania, PA 19104, USA
[2]Exxon Research and Engineering Co. Rt. 22E, Annandale, NJ 08801, USA
[3]Dept. of Applied Sciences and Dept. of Physics, Harvard University, Cambridge, MA 02138, USA
[4]National Research and Resource Facility for Submicron Structures, Cornell University, Ithaca, NY 14853, USA
[5]After Sept. 1986, Dept. of Physics, UC Santa Barbara, CA 93103, USA

Although there has been a great deal of recent activity on possible structures and some of the static properties of quasi-periodic and quasi-crystalline phases, some fundamental questions still remain about the dynamics, possibilities of commensurability and pinning, and the nature of the states for such systems. Since three-dimensional realizations of such structures, with sufficient perfection and characterization to allow meaningful studies, are not yet available, we describe some experiments on artificial two-dimensional structures which answer some of these questions experimentally. The main results are attained on superconducting networks, where the application of a magnetic field allows us to see the generalization of commensurability pinning for a variety of quasi-crystalline, quasi-periodic and disordered structures.

1. Introduction

Although there are many examples of quasi-periodicity in nature, we are just beginning to understand some of its most fundamental consequences . In particular the electronic states that one might find in a quasi-periodic potential have been under investigation for quite some time, but the exact spectra for a few well-defined models has only been available over the past 10 years [1]. Quasi-periodic potentials have often been studied as 'intermediate' between disordered and periodic. Like disordered structures they lack translational symmetry. Like periodic structures the potential can be described throughout space by specifying a few variables locally.

In quasi-periodic potentials, such as the superposition of two incommensurate sine waves, the distance between two equivalent points can take on an infinite number of values, from zero to the shorter wavelength. Recently it has been shown that quasi- periodic structures with a finite number of lengths can be mathematically constructed in any number of dimensions [2]. We will take as the definition of 'quasi-crystals' quasi-periodic potentials with a finite number of lengths. This introduces a new step in going from disordered to crystalline: disorder -> quasi-periodic -> quasi-crystal -> crystal. Recently the

discovery of an icosahedral phase of quenched AlMn [3] has led to a great deal of work on quasi-crystals.(Icosahedral symmetry is not allowed for conventional crystals, but can occur in quasi-crystals.)

Unfortunately very little is known about the spectra of quasi-periodic or quasi-crystalline systems. Theoretically the only problems which have been solved are one dimensional [4]. Experimentally there have been no detailed measurements of the spectra in any number of dimensions. There was hope that with the discovery of the icosahedral AlMn experiments could be performed on three-dimensional quasi-crystals, but as we shall see the samples are not yet of sufficient quality to allow detailed experiments. The 'novel' idea which is the nucleus of this talk is to artificially make quasi-periodic, quasi-crystalline, disordered and crystalline arrays so that the structures themselves are very well defined and then to study their physical properties. It is not easy to make large-scale structures (many basic units) of arbitrary symmetry in three dimensions, so we are limited to one or two dimensions. There already has been some work done on one dimensional quasi-crystals. Theoretically the 'Fibonacci' spectrum is known [1], and experimentally 'Fibonacci lattices' have been made by varying the spacings of multilayer structures [5]. Since we wanted to explore virgin territory we decided to work in two dimensions.

The easiest way to make two-dimensional structures of any pattern is to use a plotter connected to a computer. If you want to do more than diffraction experiments you must adapt the plotter to use other than paper and ink. In some experiments currently under way we use the plotting pen to apply epoxy dots to a rubber sheet. Then the sheet is mounted in a frame and we look at the 'drum' mode resonances. The epoxy mass loads the thin sheet and allows an evaluation of the phonon spectrum for the two-dimensional structure. It is not difficult to put down 10^3 - 10^6 epoxy plots on a 10cm x 10cm rubber sheet. It is also possible to substitute an electron beam and resist for ink and paper, and therefore microlithographically make a two-dimensional metal film. If the metal is superconducting we can perform flux quantization experiments on it and learn something about the electron spectrum using the macroscopic wavefunction of the superconductor.

2. Experiments on Icosahedrally Packed Al-Transition Metal Alloys

Before reporting on the artificial structures, we summarize what we have learned from the remarkable icosahedral phases discovered by Shechtman et al. Most of the experiments that have been published on these materials, $Al_{1-x}Mn_x$ ($x \sim 0.2$), are structural studies using electron diffraction from small crystallites or x-ray powder patterns [3,6]. The scattering studies show sharp diffraction peaks. A 'usual' interpretation would lead to a translational coherence length of the order of several hundred Angstroms. The icosahedral orientational order, however, is much larger, namely on the scale of microns. Since one interpretation of the scattering experiments is that the system is quasi- crystalline, we decided to do a number of transport, elastic and magnetization measurements.

Our most interesting result is that the resistivity is extremely high, $\rho \sim 200\ \mu\Omega$-cm $\pm$ 50% (and sometimes as high as 700$\mu\Omega$-cm), indicating

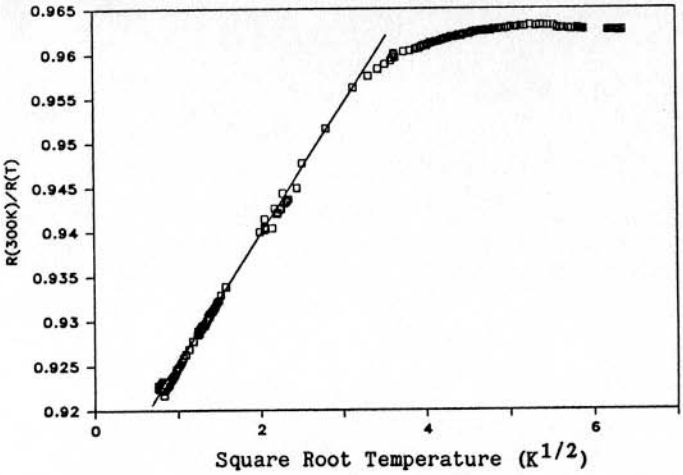

Figure 1. Low-Temperature resistivity of icosahedral phase $Al_{.8}Mn_{.2}$.

a mean free path of less than 5 Angstrom , comparable to that in a metallic glass. Moveover, from 1-10K, the conductivity decreases with decreasing temperature with a form, $\sigma = \sigma_o + AT^{1/2}$ characteristic of weak localization in three dimensions (Fig. 1). The conclusion we would like to draw from these studies is that the states in a three-dimensional quasi-crystal are weakly localized . However, the systems are sufficiently complex that it is not possible to prove this conjecture. The complications arise from a combination of the following factors: 1) Mn is magnetic in Al and in the present samples may show effects due to resonant d levels near the Fermi level E_f, spin fluctuations, the Kondo effect and the formation of a spin glass. 2) The 'stoichiometry' (x=.16-Al with some percentage of Mn, makes up an unknown (<<10%) of the samples. 3) The icosahedral phase may have substitutional disorder (e.g. as in brass). 4) The icosahedral phase may be a 'random' stacking of oriented icosahedral units rather than a quasi-crystal [7]. 5) The icosahedral phase may be a quasi-crystal with a large number of defects and/or phason strain fields.

We have eliminated many of the above objections through magnetization, thermopower and magnetoresistance measurements on a variety of samples (AlRe, AlRuMn, AlSiMn) and all of our results point to small mean free paths and weak localization. The question of substitutional disorder and the possibility of it being an icosahedral glass remain unresolved and require knowledge of the atomic positions. Nonetheless, a perturbative treatment of the low-temperature conductivity requires input simply from the structure factor S(q) and there does not appear to be sufficient diffuse scattering to account for the small mean free path.

3. Flux Quantization on Periodic Arrays

The idea of using superconductivity to probe solutions to Schroedinger's equation is an old one [8]. The superconducting order parameter has an

amplitude and a phase similar to that of a wavefunction, and in mean field is the solution to the Ginzburg-Landau equations. The minimization of the Ginzburg-Landau free energy with respect to the order parameter gives two equations, known as the GL differential equations. After linearization (appropriate at the normal-superconducting phase boundary), one of these is formally the same as Schroedinger's equation, while the other is the quantum-mechanical expression for the current due to a wavefunction.

The wavefunction - order parameter must be single valued, thus the phase integral around any closed loop must be 2π times an integer. In the presence of a magnetic field this quantization criterion becomes [9]

$$\int \nabla\phi \cdot dl = \frac{4\pi}{c\Phi_0} \int \lambda^2 J \cdot dl + \frac{1}{\Phi_0} \int A \cdot dl = 2\pi n \qquad (1)$$

where Φ_0 is the flux quantum $(hc/2e) \approx 2\times10^{-7}$ gauss-cm^2, and λ is the penetration depth. The integral over the vector potential is just the flux through the loop and the phase integral (known as the fluxoid) must always be quantized. If the magnetic field H, through the loop is exactly an integral number of flux quanta eq. 3 is satisfied with no currents circulating the loop. Then the additional kinetic energy($E \propto J^2$) is a minimum and the transition temperature is a maximum. In the case of a single circular loop $E \sim \Delta T_c \approx (\xi/a)^2 (n-\Phi/\Phi_0)^2$, where n is an integer giving the number of fluxoids in the loop, and the phase boundary is as shown in Fig. 2. This is the beautiful result demonstrated in the work of Little and Parks [9].

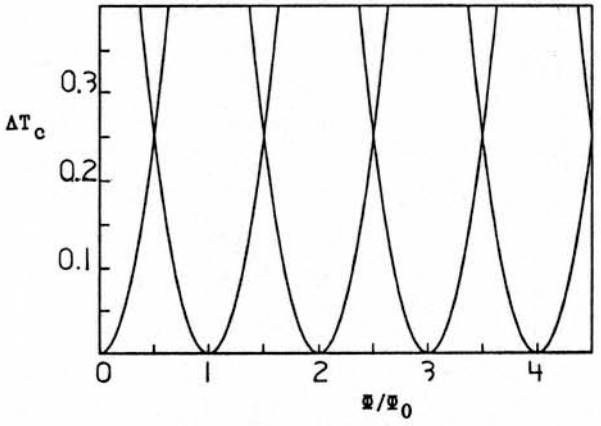

Figure 2. Decrease in transition temperature vs. flux through a single loop as in the experiment of Parks and Little[9].

The problem becomes considerably more complex when we deal with a periodic network [10]. The fluxoid is quantized on every closed path. To understand qualitatively what we might expect, it is convenient to imagine the limit where the wires which make up the network have a diameter which is much larger than the penetration depth but much smaller

than the unit cell dimensions. In the center of the wire the currents are then negligible and the flux through any closed path (through the middle of the wires) is quantized. In this limit the currents flowing on the surfaces of the wire must produce a magnetic field which makes up the difference between the applied flux and an integral number of flux quanta. The 'rules' for this simplified calculation are then current conservation at each node, and an average field for the entire network which is equal to the applied field. For example, an applied field $H<\Phi_0/a^2$ (a^2 is the area of a unit cell or an elementary tile) would correspond to a fraction f of the elementary cells having a penetrating flux quantum and (1-f) having zero flux with $f\Phi_0/a^2 = H$. The currents required for this arrangement can be calculated and the kinetic energy and ΔT_c evaluated. The experimental situation can be qualitatively recovered by realizing that the actual currents are much smaller than the ones calculated in the above approximation and the tiles containing integer flux quanta are to associated with tiles containing the same integer fluxoids. (The screening currents for most experimental situations are very small. They produce very little field modulation and to lowest order the magnetic field is uniform. However the actual currents are similar to those obtained by the recipe above and thus the T_c shift is qualitatively correct in its dependence on magnetic field.)

If we ignore correlations between occupied and unoccupied tiles (a sort of mean field treatment) then we can proceed to calculate the currents. In an applied field $H=f\Phi_0/a^2$, f cells or tiles require a current proportional to $\Phi_0(1-f)$ while (1-f) tiles require a current proportional to $\Phi_0 f$. In this situation all tiles will satisfy flux quantization. The average current is zero (as it must be to insure the average field as the applied field), however the average squared current circulating around each tile is $f(1-f)^2\Phi_0^2+(1-f)f^2\Phi_0^2=f(1-f)\Phi_0^2=\Phi(\Phi_0-\Phi)$ for $f<1$. The above arguments are easily generalized to any field and we have $\Delta T_c \sim (\Phi/\Phi_0-m)(m+1-\Phi/\Phi_0)$ for all f, (m is an integer). Thus for an infinite network ΔT_c is zero for H=0 and for $H=n\Phi_0/a^2$, but it increases linearily as H varies from these points rather than quadratically (as for the single loop problem).

The periodicity is again in terms of an integral number of flux quanta per tile but we now have cusps instead of parabolas at each minimum. The cusps result from the fact that for an infinite system when we have a field where each tile is satisfied, a slightly different field corresponds to adding a few additional widely separated flux quanta The energy cost is thus linear with the deviation from the fully satisfied case in which there are no currents.

There are additional structures at nonintegral flux quanta per tile which result from the correlations which we have neglected above. The most straightforward example is the case where $H=\Phi_0/2a^2$. If we randomly fill half of the tiles the result is $\langle J^2\rangle=1/32$. However, if we correlate the tiles with flux quanta so that they only share edges with tiles without flux (as a checkerboard for the square lattice) then the kinetic energy is decreased to $\langle J^2\rangle=1/64$. Similarly, there is a favorable correlated arrangement of the flux quanta, forming a flux lattice, for any rational fraction of a flux quantum per tile[10]. This is equivalent to having a flux lattice commensurate with the underlying periodic pattern.

A more rigorous treatment for the phase boundary of a superconducting network is found in References 11 and 12, where the linearized Ginzburg-Landau equations are treated with the constraint of current conservation at each node.

$$-\Delta_i \sum_j \cot(\theta_{ij}) + \sum_j \Delta_j e^{i\gamma_{ij}}/\sin(\theta_{ij}) = 0 \quad . \qquad (2)$$

For regular networks, with all lengths equal, the above eigenvalue problem is the same as that for an electron on a similar tight binding lattice in a magnetic field [11,12]. The eigenvalue which corresponds to the energy in Schroedinger's equation determines the coherence length, ξ, in the Ginzburg-Landau case, $\varepsilon=\cos(a/\xi)$. Since $\xi \sim \xi_o(T_{co}-T)^{-1/2}$ the maximum eigenvalue corresponds to the transition temperature. The best known example is the square lattice where the highest eigenvalue (corresponding to the Tc(H) phase boundary) is the top of the spectrum solved by Azbel and Hofstadter [13] . Again, this phase boundary shows cusps at every rational field.

We now want to see what happens when we try the same experiment on quasi-periodic or quasi-crystalline networks. In the quasi-crystalline case there are two fundamental differences from the regular periodic networks. There are at least two different tiles with irrationally related areas. It is therefore not possible to find a field which puts an integral number of flux quanta in each tile and this should dramatically affect the large-scale structure. However, the fine structure is most interesting since it relates to the 'commensurability' of the flux lattice with the network. With a quasi-periodic system it is not even clear what commensurability should mean.

4. Experiments on Quasicrystalline Arrays

The samples were fabricated at the National Research and Resource Facility for Submicron Structures at Cornell using electron beam lithography. A typical pattern consisted of 400x400 tiles with a tile area of 1-4 square microns. The network wires were aluminum, 500 Anstroms thick by 3000 Angstroms wide, deposited on a silicon wafer. The patterns were written under computer control using a Cambridge EBMF-2-150 Electron Beam Microfabricator.

Our first series of samples are 'one-dimensional' patterns consisting of a set of periodic parallel lines along y crossed by periodic, quasi-periodic, quasi-crystalline, random and several other patterns along x. The one-dimensional structures have two advantages: 1) they are considerably more variable (two or more dimensions puts constraints on many of the parameters in a quasi-crystal) and 2) it is possible to analyze the results theoretically, using the periodicity in the y direction. For the two-dimensional quasicrystal we used an eight fold generalization of a Penrose tiling. In Fig. 3 we show the optical micrographs along with the Fourier transforms of some of our networks .

In Fig. 3a is shown the 'Fibonacci' pattern which consists of two tiles with relative area τ = 1.618... (the golden mean) arranged in a Fibonacci sequence [2]. The number of large tiles is τ times the number of small tiles. The Fourier spectrum [2] consists of a dense set of

points at $(n+m\tau)/a$ reflecting the quasi- periodicity with two frequencies related by τ . In the present Fibonacci pattern all of the incommensurate ratios are given by τ. In order to distinguish the effects of quasi- periodicity from that of the irrational area ratio we have made a 'random Fibonacci' pattern, shown in Fig. 3b. The ratio of the area of the tiles is τ and there are τ times as many large as small, as in the Fibonacci. However the tiles are randomly arranged. The optical transform reflects this in showing a broad diffuse scattering instead of distinct Bragg peaks. (But there is a rather sharp spot at $q=(5/3)(2\pi/a_s)$ which comes from the Hendricks-Teller effect.[14])

The phase boundary $T_c(H)$ for the Fibonacci and random Fibonacci patterns are shown in Fig. 4. A quadratic background due to the finite thickness of the aluminum wires has been subtracted. It is immediately clear that neither pattern is periodic and that, although similar in

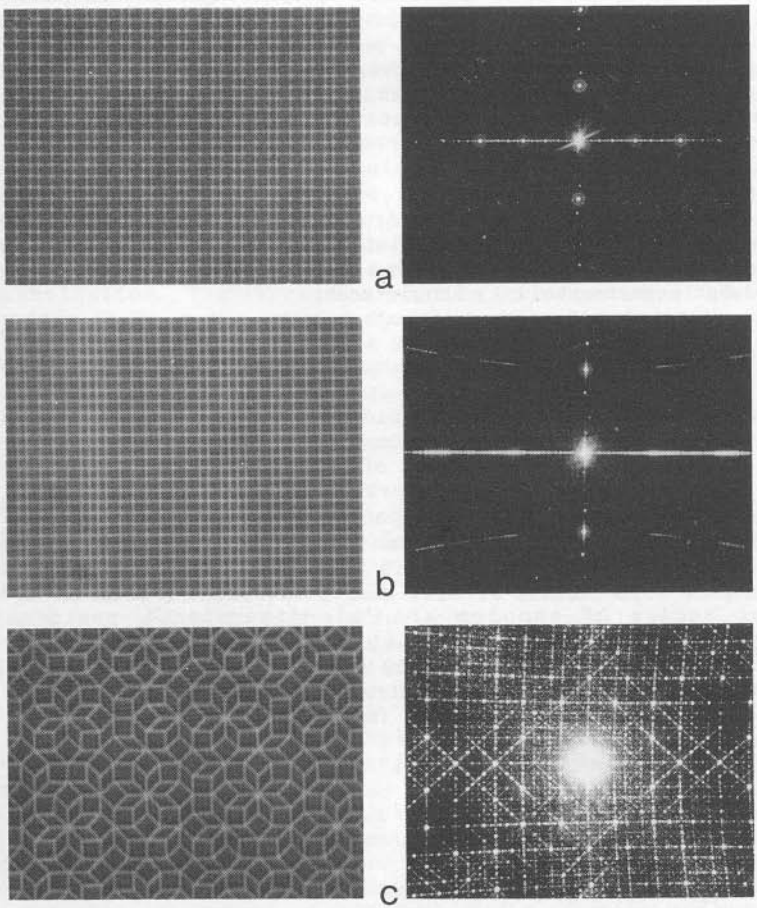

Figure 3. Optical Micrographs and Optical diffraction patterns for: a) 'Fibonacci Lattice', b) 'Random Fibonacci, c) 'Eight-fold Penrose Tiling'.

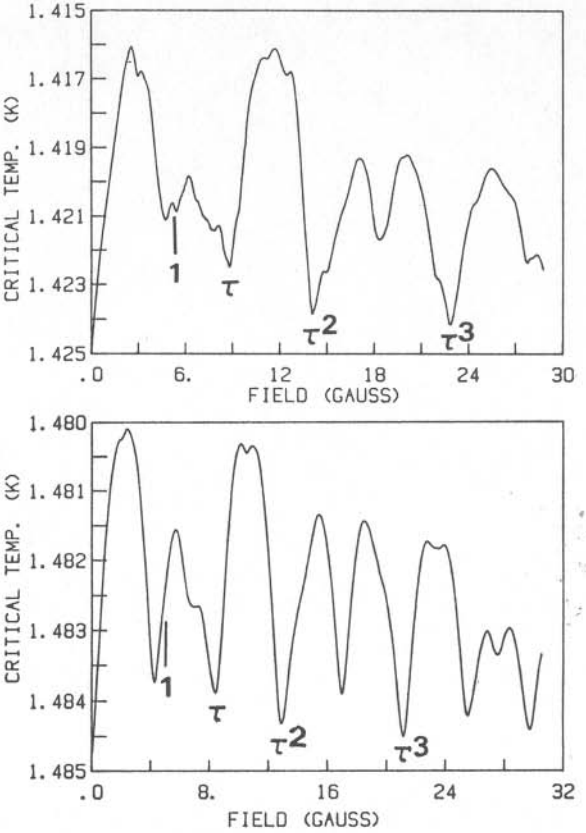

Figure 4. Experimental data on the phase boundary for a) the Fibonacci Lattice and b) the Random Fibonacci pattern.

gross features, they are different in detail. In particular there are large dips in both curves which, in analogy to the periodic network, should reflect the area or areas of the tiles. However there is no fine structure in the random Fibonacci and a lot of fine structure in the Fibonacci. This immediately tells us that the quasi- periodicity is important and that the flux lattice has found a way to be commensurate with the quasi- crystal.

The large-scale structure in both Fibonacci and random Fibonacci is easy to understand. The transition temperature for a given field would return to zero-field value if we could put an integral number of flux quanta in each tile [10]. In the infinite field limit we could do this. For finite fields we can approximate flux quantization at fields which correspond to rational approximates to τ (M/N=1,2,3/2,5/3,8/5,13/8, etc.). If we put M flux quanta in the small tiles and N in the large tiles then the average field is $H=(M+N\tau)/(1+\tau^2)$. For the low rational approximates (M,N) = (1,1), (1,2), (2,3), (3,5), (Fn,Fn+1), corresponding to applied fields of $M/Ho = 1, \tau, \tau^2, \tau^3, \ldots, \tau^n$ where $Ho = \Phi_0/a_s^2)(1+\tau)/(1+\tau^2)$. H_0 is the field which corresponds to one flux quantum in each tile. Thus the largest structures which

occur in $T_c(H)$ for both Fibonacci and random Fibonacci are again related to the properties of the elementary tiles.

In order to proceed further we turn to the network equations of references 11,12. It is a straightforward matter to write down the coupled equations for the Fibonacci sequence using its generating function $x_m=m+(1/\tau)\mathrm{INT}(m/\tau)$, defining $\Delta_m=x_{m+1}-x_m$, and using equation 2

$$\Lambda_{mn}[\,2\sin(\tau a/\xi)\cos(a/\xi) + \cot(\Delta_{m-1}a/\xi)\sin(a/\xi)\sin(\tau a/\xi)$$

$$+ \cot(\Delta_m a/\xi)\sin(a/\xi)\sin(\tau a/\xi)\,]$$

$$-\sin(a/\xi)\sin(\tau a/\xi)[\Lambda_{m-1,n}/\sin(\Delta_{m-1}a/\xi) + \Lambda_{m+1,n}/\sin(\Delta_m a/\xi)]$$

$$-\sin(\tau a/\xi)[\Lambda_{m,n+1}\exp(i\gamma x_m a) + \Lambda_{m,n-1}\exp(-i\gamma x_m a)] = 0 \quad . \qquad (3)$$

We are using a Landau gauge, (0,Hx), with $\gamma=eH/hc$. The only place where a 'y' dependence enters the equation is in the last terms on the right, involving the nodes m,n+1 and m,n-1. The form is such that the solution must merely contain a Floquet factor and hence the problem reduces to one dimension. However the eigenvalue problem still needs computer solutions. Evaluated on a 23x23 network we find the normalized phase boundary shown in Fig. 5. The computation reveals the major dips at factors of τ predicted above and some of the fine structure seen in the experiment. In fact the calculation fits the experiment remarkably well although the experiments have finer structure. An additional feature which appears in the calculation is a quasi mirror symmetry about the points $(\tau^n+\tau^{n+1})/2$ which extends from 0 to $\tau^n + \tau^{n+1}$ [15].

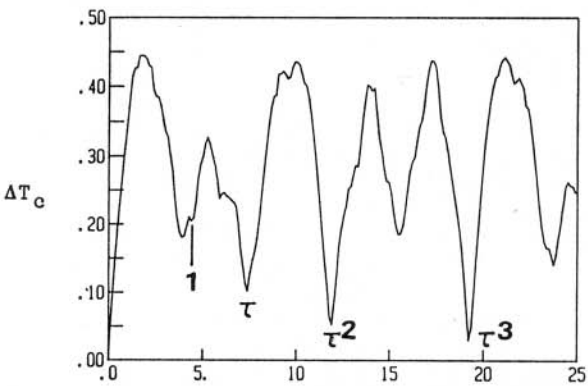

Figure 5. ΔT_c vs. Φ/Φ_0 calculated from the linearized GL equations for the Fibonacci Lattice.

The Fibonacci and the Random Fibonacci patterns tell us much that we want to know about flux quantization in quasi-periodic networks. The features due to the areas of the tiles dominate the phase boundary and the main dips which were at $n\Phi_0/a^2$ for the periodic case now vary as $(\Phi_0/a^2)\tau^n$. We have also seen that fine structure is present only in the ordered quasi-periodic network indicating the importance of the long range coherent structure for the flux lattice commensurability. This

'locking in' of the flux lattice is also indicated by the important observation that many dips in the Fibonacci lattice are 'cusp-like', while those in the random Fibonacci are all quadratic. Unfortunately the interpretation of each dip in the 'one-dimensional' patterns is difficult , because the periodicity along y actually complicates a simple labelling scheme.

Our two-dimensional quasi-crystal is the eight fold version of a Penrose tiling (a Penrose tile could not be fabricated since the E - Beam Fabricator cannot draw lines at 72^{o} angles), fig. 3c. It consists of two tiles, a fat and a skinny, with area ratio $\Omega=2^{\frac{1}{2}}$. Unlike the Penrose tiling there are more skinnies than fats by the ratio Ω . However the quasi-periodicity is characterized by the number $\sigma=1+\Omega$, that is the pattern is generated by an inflation scheme with each inflation changing characteristics distances by σ. The average field for N_f (N_s) flux quantum in every fat (skinny) tile is $H=(\Omega N_s+N_f)\Phi_o/(2\Omega)A_s=(\sigma)\Phi_o/(2\Omega)A_s$. We expect the biggest effects for rational approximates to the area ratio $\Omega=2^{\frac{1}{2}}$. The lowest few are the pairs $(N_f, N_s) = (1,1), (3,2), (7,5)$ which correspond to average fields $H/Ho=1,\sigma,\sigma^2$ as indicated in Fig. 6. It is interesting that the parameter that comes in when we are trying to rationalize the area ratio Ω, is the quasi-periodicity ratio σ. This is of course not accidental, but comes from the restrictions in forming quasi-crystals.

Aside from the 'major dips' there are smaller dips between the values $H/Ho = \sigma^n$. These dips correspond to the flux lattice finding favorable configurations on the quasi-crystalline substrate. There should of course be dips everywhere, but the largest ones in the present case can be readily indexed by $H(n,m) = Ho(n+m\sigma)$ with n,m positive and

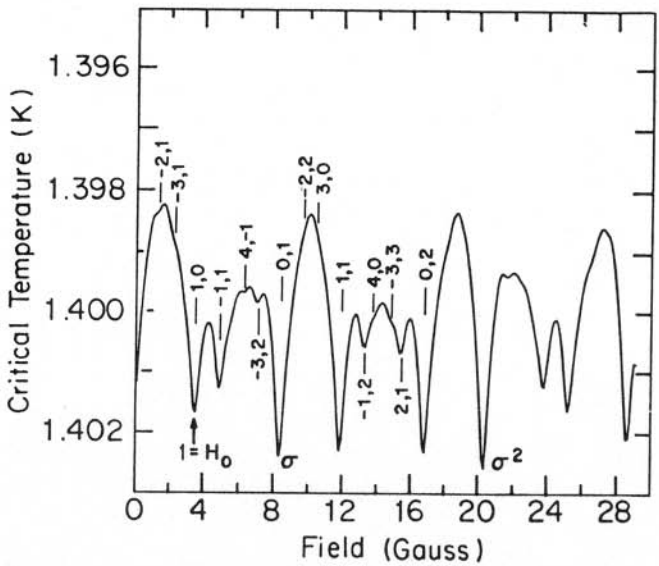

Figure 6. Experimental Data on the transition temperature vs. applied field for the 'Eight fold Penrose tiling'.

negative integers. The combination which yields fields less than σ^2 with n,m less than 4 are shown in Fig. 6. Most are readily identified. Thus the system which replaces the rational fields H = (p/q)Ho for the periodic structure is H=Ho(n+mσ) for the quasi-crystalline networks. It is worth pointing out that for quadratic irrationals, say β, p/q is in general not a member of n+mβ, whereas $s\beta^t$ is a member (n,m,p,q,s,t integers). Thus some combinations of n+mσ may be viewed as deflations of the quasicrystal. It is not unreasonable that a flux lattice may lock in or show epitaxy with a deflation of a quasi-crystalline network.

Our results on the 'Fibonacci' sample and the eight-fold Penrose tiling suggest the generalization of the concept of commensurability to include superstructures on whose Fourier transform the fourier transform of the original structure is completely found. This definition works equally well for the sparse points which are the reciprocal lattice for conventional crystals and the dense points which form the diffraction pattern of quasi-crystals.

Unfortunately we cannot calculate the expected phase boundary for the two-dimensional patterns. As discussed earlier the problem is equivalent to solving the electronic structure which is not yet possible. However we see that the main features are similar to what has been seen in the one-dimensional quasi- crystals: large dips at σ^n, fine structure and the remarkable quasi-reflection symmetry about $(\sigma^n+\sigma^{n+1})/2$.

The use of artificial structures and in particular superconducting networks can be useful for studying the properties of other patterns as well. Self-similar ordered fractals such as Sierpinski gaskets have been made [16] and random fractals such as percolation clusters are being studied along with quasi-periodic systems.

In conclusion,we have prepared a series of superconducting networks in the form of periodic, quasi- periodic , quasi- crystalline and disordered patterns. Our main result from this study is that a flux lattice can be commensurate with a quasi-crystal. This implies that it should be possible to grow epitaxially (at other than the trivial 1:1 case) on a quasi- crystalline substrate. We have also shown the utility of such artifical patterns for gaining insight into some unsolved problems in new structures with unusual symmetries and construction.

Part of this research is supported by NSF under grants DMR83-18060 (M. J. B.) and through the Laboratory for Research on the Structure of Matter, DMR85-19059 (A. B.)

References

1. S. Ostlund and R. Pandit: Phys.Rev B 29, 1394 (1984)
2. D. Levine and P.J. Steinhardt: Phys.Rev. Lett. 53, 2477 (1984)
3. D. Shechtman, I. Blech, D. Gratias, and J.W. Cahn: Phys. Rev. Lett. 53 , 1951 (1984)
4. B. Simon: Adv. Appl. Math. 3, 463 (1982).
5. R. Merlin, K. Bajema, R. Clarke, F.-Y. Juang, and P.K.Bhattacharya: Phys. Rev. Lett. 55, 1768 (1985)
6. P.A. Bancel, P.A. Heiney, P.W. Stephens, A.I. Goldman, and P.M. Horn: Phys. Rev. Lett. 54 ,2422 (1985)

7. P.W. Stephens and A.I. Goldman: Phys. Rev. Lett.56 ,1168 (1986)
8. V. L. Ginzburg and L. D. Landau, Zh. Eksperim. i Teor. Fiz 20, 1064 (1950).
9. R.D. Parks and W.A. Little: Phys. Rev. A133, 97 (1964)
10. B. Pannetier, J. Chaussy, R. Rammal,and J.C. Villegier: Phys.Rev.Lett. 53, 1845 (1984)
11. S. Alexander: Phys. Rev.B 27, 1541 (1983)
12. R. Rammal, T.C. Lubensky, and G. Toulouse: Phys. Rev.B 27 ,2820 (1983)
13. M. Ya. Azbel: Zh. Eksp. Teor. Fiz. 46, 939 (1964) [Sov. Phys. -JETP 19 ,634 (1964), D.R. Hofstadter: Phys. Rev. B14, 2239 (1976)
14. S. Hendricks and E. Teller, J. Chem. Phys. 10, 147 (1942).
15. A. Behrooz, M. J. Burns, H. Deckman, B. Whitehead, and P. M. Chaikin, Phys. Rev. Lett. 57, 368 (1986).
16. J. M. Gordon, A. M. Goldman, J. Maps, D. Costello, R. Tiberio and B. Whitehead, Phys. Rev. Lett. 56, 2280 (1986).